JURNAL rekayasa mesin
Vol. 16. No.1
ISSN 2477-6041 articles 23, pp. 267 – 282, 2025

DESIGN AND ANALYSIS OF AN AXIAL FLUX PERMANENT MAGNET GENERATORS WIND TURBINE FOR AUTOMATIC STACKING CRANES

Aisyah Aira Putri Maharani [1]✉, Muhamad Rizalul Wahid [1], Mahmudah Salwa Gianti [1], Tri Seda Mulya [1], Ari Rahayuningtyas [2]

[1] **Department of Mechatronics and Artificial Intelligence**
Universitas Pendidikan Indonesia
Bandung, INDONESIA
Jl. Dr. Setiabudi 229, 40154
aisyahairaputrim@upi.edu
rizalulwahid@upi.edu
msg.salwa@upi.edu
trisedamulya929@upi.edu

[2] **Badan Riset dan Inovasi Nasional**
Directorate for Laboratory Management, Research Facilities, and Science and Technology Park.
Subang, INDONESIA
JL. K.S Tubun 5, 41211
arirahayuningtyas@gmail.com

Abstract

Automatic Stacking Cranes are indispensable tools in modern ports that can transfer containers between the landside and the waterside. These cranes are powered by electricity and consume significant amounts of energy to meet annual production demands. This substantial electricity consumption often strains the port's power grid during voltage and current fluctuations, which can destabilize the ASC's power supply. Wind turbines offer a promising alternative energy source to address these problems. This study delves into the analysis of the optimal Axial Flux Generator structure for wind turbines and calculates the associated energy losses to determine the feasibility of a wind turbine system capable of supporting the ASC's power demands. The findings reveal that employing an AFG-based wind turbine can generate the required 88,497 Watts of power for the ASC, with an average rotational speed of 1,655 rpm. This represents an annual electricity cost saving for the port of approximately 39,701,029 Rupiah.

Keywords*: Automatic Stacking Cranes, Axial Flux Permanent Magnet Generator, Energy Efficiency, Wind Turbine*

1. INTRODUCTION

Automatic Stacking Cranes (ASCs) have become indispensable components in modern port operations, playing a pivotal role in the efficient and seamless movement of containers between landside and seaward areas [1]. These cranes perform a combination of lifting, shifting, and stacking operations to ensure the orderly arrangement of containers within the port environment. Crucially, ASCs are complemented by yard panels, which serve as essential components in their operation [2]. Yard panels facilitate automated control of ASC movements, integrating seamlessly with the port's Terminal Operating System (TOS). This integration enables ASCs to receive and execute container stacking commands with precision and efficiency. The integration of ASCs and yard panels within the TOS framework streamlines container handling operations, optimizing yard utilization and enhancing overall port productivity. This collaborative system contributes significantly to the smooth flow of cargo through the port, minimizing delays and ensuring timely deliveries [3].

ASCs primarily rely on electricity from the national grid (PLN) as their main power source. This presents a significant advantage as it ensures a continuous and sustainable supply of energy. Additionally, electricity has minimal energy loss, effectively meeting

Corresponding Author:
✉ **Aisyah Aira Putri Maharani**
Received on: 2024-10-25
Revised on: 2025-02-05
Accepted on: 2025-03-19

DOI: 10.21776/jrm.v16i1.1984

the crane's power requirements [4]. However, the use of PLN electricity also poses certain challenges, particularly in terms of dependency. Any disruptions to the PLN supply, such as power outages, short circuits, or maintenance, can severely hinder the ASC's operations. Furthermore, the substantial energy consumption of ASCs, estimated at around 60,000 Watts, can strain the overall power grid within the port. This situation poses potential safety hazards, as disruptions to ASC operations can indirectly impact other critical port equipment [5]. For instance, Ship to Shore cranes, responsible for transferring containerized cargo between ships and land, and Grab Ship Unloaders, tasked with moving dry bulk cargo from ships to land, can also be affected. Conversely, issues can also arise when the terminal's power grid experiences instability, particularly during voltage and current fluctuations. These conditions can prevent Automatic Stacking Cranes from operating at their peak performance [6].

Wind turbine emerges as a compelling solution to address the pressing these energy challenges. This ingenious device harnesses the kinetic energy of wind, a renewable energy source, to drive generators and produce electricity [7], [8]. Its holds immense potential, particularly for coastal terminals situated in areas with consistently high wind speeds averaging 13 m/s [9]. However, a key challenge lies in the fluctuating wind direction, as air currents tend to move in various directions. When land temperatures surpass sea temperatures, winds originate from the ocean and flow towards the land, and vice versa. This variability in wind direction poses a challenge for conventional wind turbines, as it hinders the consistent and efficient generation of electricity. To address this challenge, innovative wind turbines are required that can effectively adapt to fluctuating wind directions, ensuring optimal energy capture. These advanced turbines will play a pivotal role in unlocking the full potential of wind energy, particularly in coastal regions with abundant wind resources.

In light of these considerations, an effective wind turbine system is required to generate electricity that can meet the diverse power needs of Automatic Stacking Cranes (ASCs). This study will investigate the optimal structural analysis of Axial Flux Permanent Magnet Generators (AFPMGs) to ensure the efficient operation of wind turbines. The study will also meticulously examine the calculation of associated energy losses to determine the feasibility of wind turbine systems in effectively supporting the power requirements of ASCs. This approach represents a more environmentally friendly solution for power supply without disrupting the operation of other equipment.

2. LITERATURE REVIEW

2.1. Automatic Stacking Crane

ASCs are indispensable tools in the realm of container handling, revolutionizing the industry with their ability to operate autonomously [10]. While manual control remains an option, ASCs primarily function without human intervention, enhancing efficiency and safety. Gantry Crane, the towering structure that forms the ASC's backbone, mounted on rails for smooth movement along designated paths. Hoist, the muscular heart of the ASC, responsible for lifting and lowering containers with precision and power. Trolley, a nimble traveler, traversing the gantry crane's bridge to precisely position the hoist over the containers awaiting their journey [11]. Electrical panels are the main soul for supplying electricity to the various components of the stacking crane that includes the hoisting mechanism, drive systems, and control systems. This also ensures that all parts function efficiently and safely.

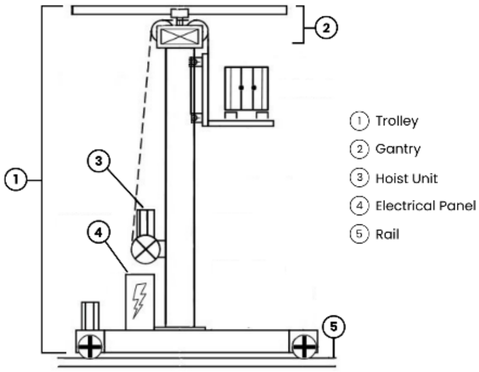

Figure 1. Main component of automatic stacking crane.

2.2. Wind Turbine

Wind turbines are crucial components of Wind Energy Conversion Systems (WECS) [12]. These turbines harness the kinetic energy of the wind to generate mechanical energy in the form of shaft rotation. This rotational energy is then utilized to drive a generator for electricity production [13]. Based on the rotor configuration, wind turbine designs are categorized into two primary types: horizontal axis wind turbines (HAWTs) and vertical axis wind turbines (VAWTs) [14].

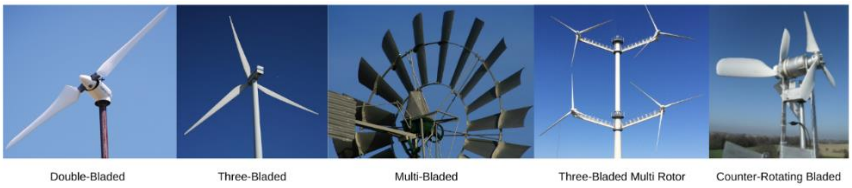

Figure 2. Type of horizontal axis wind turbine

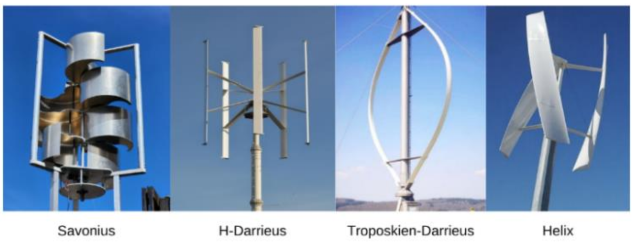

Figure 3. Type of horizontal axis wind turbine.

2.3. Axial Flux Permanent Magnet Generators

Axial flux permanent magnet (AFPMG) generators operate on the same fundamental principle as conventional generators, but with a key distinction in the direction of flux flow [15]. In AFPMGs, the flux lines cut through the stator axially rather than radially. This unique flux path allows AFPMGs to achieve a significantly more compact design, resulting in a superior power density (output power per unit mass/volume) compared to conventional generators.

An axial flux permanent magnet generator (AFPMG) also known as a pancake generator, is characterized by its unique design where the components are arranged by housing and cover as the structural framework that supports the rotor and stator while protecting the internal components from environmental factors [16]. Two rotors, that look like a flat disk that houses the permanent magnets for creates an alternating magnetic field that interacts with the stator coils and inducing electrical current. Permanent magnets, a crucial component of the AFPMG for creating a magnetic field that induces voltage as the rotor spins. Stator, the stationary component that contains the windings for balance axial forces and improve cooling. Windings, the part to generate higher induced voltage when exposed to the changing magnetic field of the rotor [17].

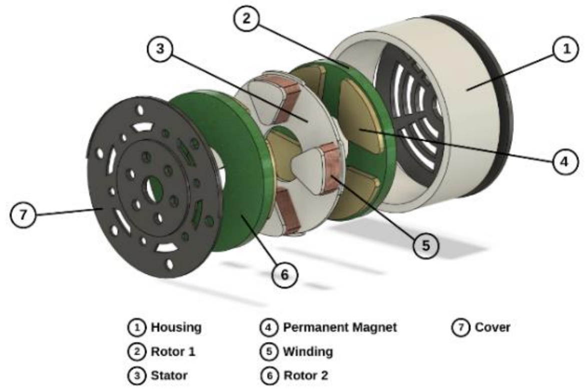

Figure 4. Structure of axial flux permanent magnet generator.

3. METHOD

3.1. Wind Turbine Design

The wind turbine design employs a vertical axis wind turbine (VAWT) as illustrated in Figure 5. This type was selected for its superior efficiency compared to its horizontal axis counterpart [18]. VAWTs are also well-suited for areas with unpredictable wind directions [19]. Overall, the advantages of VAWTs over HAWTs, which informed the design decision, are as follows:

1. VAWT can capture more stable winds from all directions.
2. VAWT has a simpler construction
3. VAWT is suitable for installation in terminal areas even with minimum wind speeds.
4. Lower maintenance costs

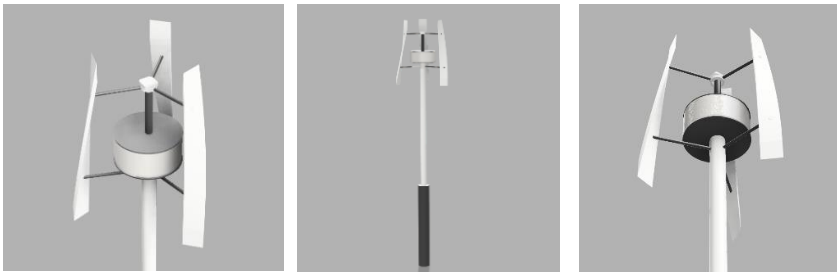

Figure 5. Design of vertical axis wind turbine.

To achieve better force distribution and balance, this design employs a Helix-type blade as shown in Figure 6. This blade ensures that during turbulence, wind can still act on every part of the surface area, resulting in higher efficiency from incoming wind compared to other vertical axis wind turbines [20]. This type is also known for its quiet operation, as the blade tips move at slower speeds, reducing noise pollution. The minimum wind speed required for this type to rotate is 3–7.5 m/s [21].

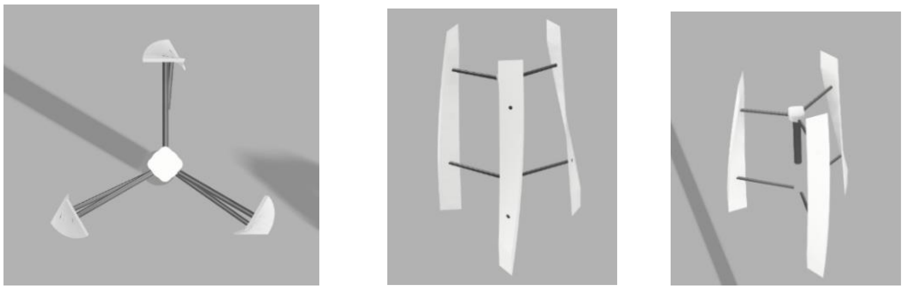

Figure 6. Design of vertical axis wind turbine.

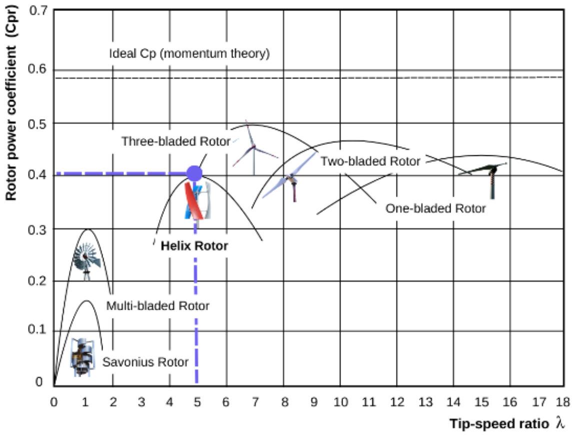

Figure 7. Comparison curve between tip speed ratio (TSR) and rotor power coefficient (RPC).

This blade exhibits a power coefficient (Cp) of 0.4 and a tip speed ratio (TSR) of 5, as illustrated in Figure 7. A Cp value of 0.4 is considered high, indicating efficient conversion of wind energy into electrical energy [22]. Similarly, a TSR of 5 is deemed optimal for many modern wind turbines. The combination of a high Cp and an optimal TSR suggests that the helical-type turbine design effectively captures and converts wind energy, making it a reliable renewable energy source. Based on the TSR value, Table 1 indicates that three blades are employed [23].

Table 1. Relationship between TSR and number of blades.

TSR	Number of Blades
1	8-24
2	6-12
3	4-6
4	3-4
>4	1-3

3.2. Axial Flux Permanent Magnet Generator Design

3.2.1. Permanent Magnet

This design utilizes Neodymium-Iron-Boron (NdFeB) magnets, composed of an alloy of neodymium, iron, and boron, forming the Nd2Fe14B tetragonal crystalline structure [24]. These magnets outperform other permanent magnets like Ferrite, Alnico, and Samarium Cobalt due to their superior magnetic induction and magnetic field strength. NdFeB magnets boast a magnetic induction of 1.2 T and a magnetic field of 900 Ka/m, as demonstrated by the demagnetization curve in Figure 10. Additionally, NdFeB magnets exhibit a remarkable maximum energy product (BH_{max}) of 30 – 52 MGOe, far exceeding the maximum energy product of Ferrite magnets, which ranges from 0.92 – 3.5 MGOe [25]. Due to its high effectiveness, this type of permanent magnet is widely used in various industrial applications, including electronic devices, sensors, and transducers. Moreover, it is primarily employed in generators to produce a strong and stable magnetic field [26].

This, in turn, enhances the efficiency of electromagnetic induction in converting kinetic energy into electrical energy with minimal losses.

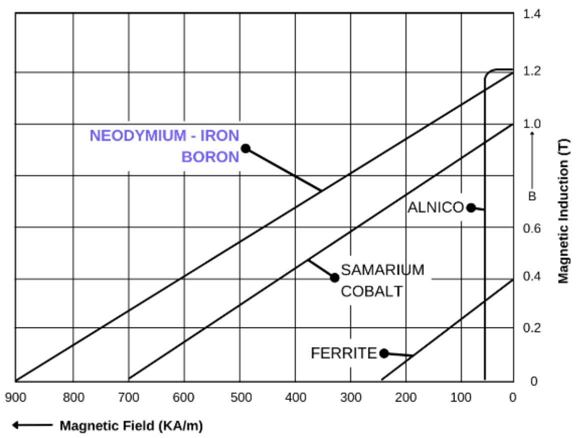

Figure 8. Demagnetization curve.

3.2.2. Generator Speed

The rotational speed of a generator's rotor measured in revolutions per minute (rpm) is a crucial factor in determining the generator's electrical output. This rotation process converts mechanical energy into electrical energy through electromagnetic induction [27]. To calculate the required number of rotations, the number of magnetic poles and the utilized electrical frequency must be considered. This rotational speed ultimately influences the generator's output voltage [28]. The equation below describes the relationship between these parameters (1).

$$n = \frac{120\, f}{p} \tag{1}$$

Based on Hutte's standards [29], the relationship between the number of poles and the number of revolutions for a frequency of 50 Hz is summarized in Table 2. In various cases, the number of revolutions affects the power output. The higher the number of revolutions, the greater the power output. Therefore, for this design, the number of revolutions is set to 1,500 rpm. As shown in Table 2, this corresponds to 4 poles.

Table 2. Relationship between number of poles and generator speed.

Number of Poles (p)	Number of Speed (rpm)
2	3,000
4	1,500
6	1,000
8	750
10	600
12	500
16	375
20	300

3.2.3. Calculation of Current per Stator Phase

Stator phase current is the electrical current flowing through each phase of the stator winding in a three-phase generator [30]. The current flowing through each stator phase is responsible for generating a rotating magnetic field that interacts with the rotor's magnetic field to produce torque or electromotive force (EMF) for machine operation. The magnitude of the stator phase current is influenced by the load connected to the generator, the applied voltage, and the coil impedance. This current must be carefully monitored to ensure efficient operation and prevent overheating or damage to the system.

The magnitude of the stator phase current can be calculated using the equation (2) is I_a = 126.26 A ≈ 126.3 A, assuming an output power of 75,000 Watts, a power factor of 0.9, and three phases, the stator phase current can be calculated as follows [31].

$$I_a = \frac{P_{out}}{m_1 \times V_1 \times cos\theta} \quad (2)$$

3.2.4. Stator Outer Diameter Calculation

Stator outer diameter is the physical dimension of the stator's outermost surface in a generator [32]. This diameter is crucial in determining the overall size of the machine and influences the design and placement of other components. An appropriate outer diameter can impact electromagnetic performance and the generated torque. The stator outer diameter obtained using Equation (3) is 0.469 meters, as illustrated in Figure 9 [31].

$$D_{out} = \sqrt[3]{\frac{\varepsilon \times P_{out}}{\pi^2 \times K_D \times K_{W1} \times n \times B_{mg} \times A_m \times \eta cos\,\theta}} \quad (3)$$

Parameters	**Value**
Voltage ratio (ε)	0.9
Distribution factor (K_D)	0.1312
Winding factor (K_{W1})	0.96
Rotation (n)	25 rad/s
Flux density value (B_{mg})	0.65T
Current density value (A_m)	40,000 A/m
Power factor (cos θ)	0.9
Efficiency (η)	90 %

3.2.5. Stator Inner Diameter Calculation

The inner diameter of the stator is the dimension of the inner side of the stator that surrounds the rotor in a generator. This diameter is crucial as it determines the clearance between the stator and rotor, which impacts the overall efficiency and performance of the machine [33]. The inner diameter of the stator must be large enough to allow the rotor to rotate smoothly without excessive friction or contact, yet small enough to ensure that the magnetic field generated by the stator coils can effectively interact with the rotor. The chosen value for the inner diameter of the stator is D_{in}= 0.270 meters, based on Equation (4) as shown in Figure 9 [31].

$$D_{in} = \frac{D_{out}}{\sqrt{3}} \quad (4)$$

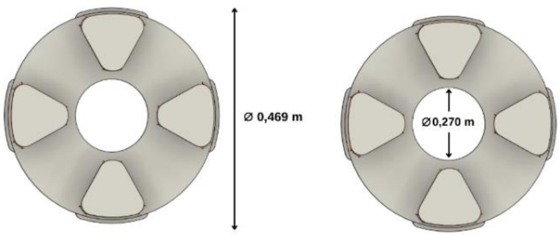

Figure 9. Design of the stator a) Outer b) inner.

3.2.6. Stator Magnetic Flux Calculation

Stator magnetic flux is the total number of magnetic field generated by magnetic field lines that pass through the stator coils in a generator [34]. This flux is generated by the electric current flowing through the stator coils and is a key component in the electromagnetic induction process that converts mechanical energy into electrical energy or vice versa. A strong and well-directed stator magnetic flux enables effective interaction with the rotor, producing the electromotive force (EMF) or torque required for machine operation. Managing and optimizing stator magnetic flux is crucial for ensuring generator efficiency, performance, and reliability. Based on the following equation (5) [31], assuming a value of $2/\pi$ for $\propto$i, a number of poles (p) of 4. Therefore, the stator magnetic flux is approximately 0.00597 Wb [31].

$$\emptyset f = \propto i \times B_{mg} \times \frac{\pi}{2p} \times [(0.5 \times D_{out})^2 - (0.5 \times D_{in})^2] \quad (5)$$

3.2.7. Calculation of the Number of Windings per Stator Phase

Stator phase turns represent the number of wire coils on each phase of the stator in a generator [35]. Each stator phase has a specific number of turns designed to generate a magnetic field when electric current flows through it. The number of turns directly impacts on the strength of the generated magnetic field, as well as the voltage and current induced in the rotor. Properly designed stator phase turns ensure that the electric machine operates efficiently and meets the desired performance specifications. Additionally, an optimal number of turns aids in controlling the generated heat, reducing energy losses, and enhancing the durability and lifespan of the electric machine. The number of stator phase turns can be calculated using equation (6) which assuming a phase voltage (E) of 220 volts and a frequency (f) of 50 Hz, Therefore the number of stator phase turns is N_1= 174.48 ≈ 175 turns [31].

$$N_1 = \frac{E}{4.4 \times f \times K_{W1} \times \emptyset f} \quad (6)$$

Figure 10. Design of stator with coils.

3.2.8. Calculation of Stator Conductor Cross-sectional Area

Stator conductor cross-sectional area is the measurement of the transverse area of the conductor wire used in the stator windings of a generator [36]. This area is crucial as it influences the conductor's ability to carry electrical current without generating excessive heat. Selecting an appropriate cross-sectional area involves considering the current that will flow through the conductor, the conductor material, and cooling requirements. An optimal cross-sectional area helps maintain safe operating temperatures, prevents insulation breakdown, and extends the lifespan of the electrical machine by ensuring the conductor can effectively handle the electrical load. The calculated stator conductor cross-sectional area is S_a= 7.016 mm2, considering the number of parallel wires a_w= 4 and the stator conductor current density (J_a) = 4.5×106 A/m2, as per the provided equation (7) [31].

$$S_a = \frac{I_a}{a_w \times J_a} \quad (7)$$

3.2.9. Rotor

Permanent magnets on the rotor are arranged in alternating north and south poles to generate a magnetic flux due to the attractive forces between them [37]. The inner diameter (D_{in}) and outer diameter (D_{out}) of an axial flux generator rotor are equal to the inner and outer diameters of the stator, respectively. In this case, as shown in Figure 11, the inner diameter (D_{in}) is 0.270 meters, and the outer diameter (D_{out}) is 0.469 meters.

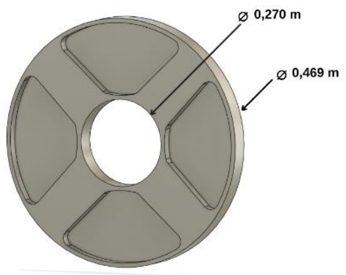

Figure 11. Design of rotor.

4. RESULTS AND DISCUSSION

4.1. Copper Loss Calculation

Copper losses are a type of energy loss that occurs in generators. These losses arise due to the electrical resistance of the copper material used to make the windings (coils) or conductors in these components [38]. When electric current flows through copper windings or conductors, some energy is dissipated as heat due to electrical resistance. The higher the current flowing, the more heat is generated. This can lead to several negative effects, such as reduced efficiency and increased temperature. Therefore, it is necessary to calculate copper losses using equations (8) and (9) [31].

$$\Delta P_{1W} = m_1 \times I_a{}^2 \times R_1 \tag{8}$$

$$R_1 = \frac{N_1 \times L_{1av}}{a_w \times \sigma \times S_a} \tag{9}$$

With:

ΔP_{1W} = Copper loss (Watts)
L_{1av} = Stator wire length (m)
N_1 = Number of windings per phase of stator
I_a = Stator winding current (A)
R_1 = Stator winding resistance (Ω)
σ = Electrical conductivity of copper

By entering the parameter values $L_{1av} = 0.6766$ m, $\sigma = 57 \times 10^6$, then the stator winding resistance is obtained $R_1 = 0.0758132\ \Omega$, so that the amount of copper losses obtained is $\Delta P_{1W} = 3{,}628$ Watts. This copper loss still needs to be added with other losses based on the equation (10), so that the overall copper total loss is obtained 4,353 Watts.

$$\Delta P_{stray} = 20\% \times P_{1W} \tag{10}$$

4.2. Friction and Wind Losses Calculation

Friction and windage losses are two types of mechanical losses that occur in generators. They result from the interaction of rotating components with their surroundings and contribute to a reduction in generator efficiency [39]. Friction losses arise from the direct contact of moving parts within the generator, such as bearings and brushes. This interaction generates frictional forces that oppose the rotation, leading to energy dissipation in the form of heat. The magnitude of friction losses depends on factors like the material properties of the components, the applied pressure, rotational speed, and lubricant viscosity. Windage losses stem from the aerodynamic drag experienced by rotating components as they interact with air. This resistance creates a frictional force that counteracts the rotational motion, slowing it down and dissipating energy. Windage losses are particularly significant at high rotational speeds, where air resistance increases proportionally with the square of the speed. This indicates that these losses account for a power loss of 583.333 Watts. Minimizing friction and windage losses is crucial for improving generator efficiency and reducing energy waste. This can be achieved through careful design, material selection, lubrication, and proper ventilation (11) [31].

$$\Delta P_{f\&w} = 0.7\% \times \frac{P_{out}}{cos\theta} \quad (11)$$

4.3. Energy Efficiency Calculation

The amount of efficiency obtained is η = 94.96% where equation (12) is used [31].

$$\eta = \frac{P_{out}}{P_{out} + \Delta P_{1w} + \Delta P_{stray} + \Delta P_{f\&w}} \times 100\% \quad (12)$$

The efficiency value produced in this design is 4.96% greater than that found in the initial calculation parameters in equation (3) which is 90%. This increase is certainly very significant. This increase indicates that the loss calculation is much more optimal. The maximum loss calculation results in a smaller overall loss value compared to the calculation contained in the parameters of equation (3). This smaller value is the main reason for the increase, because the magnitude of the loss value is inversely proportional to the efficiency value. The smaller the loss generated, the greater the efficiency obtained, and vice versa [40].

The loss value is also related to the calculation of the stator and rotor design. In the calculation of losses, there is the role of calculations regarding the stator winding current, the number of turns per stator phase, and the cross-sectional area of the conductor that has been done before. The amount of stator winding current, the number of turns per stator phase, and the conductor cross-sectional area are also influenced again by many other things such as the load connected to the generator, the applied voltage, coil impedance, frequency, current density, and many others. This indicates that each calculation in this design is interrelated so as to successfully produce a permanent magnet axial flux generator with accurate specifications.

Increased efficiency values result in a wide variety of benefits. With higher efficiency, wind turbines can generate more electricity from the same wind speed [41]. This means the output generated by the turbine will increase to produce more energy for consumption. Higher efficiency can also reduce the cost per unit of Automatic Stacking Crane panel yards which previously cost a lot of electricity consumption due to increasing production needs.

4.4. Output Power Calculation

The amount of efficiency panel of the Automatic Stacking Crane. Generally, there are 20 ASCs in a terminal to support the terminal operational process. One Automatic Stacking Crane is supported by 1 yard panel.

Output power is obtained based on the existing wind speed at the Port. From reference [26] the minimum speed at which the wind blows is 7 m/s with the average speed is 13 m/s. So therefore, based on the equation (13), generator obtained a power of 900.375 Watts for wind speed at 7 m/s and 5,767 Watts for average wind speed 13 m/s.

$$P = \frac{1}{2} \times \rho \times A \times V^3 \quad (13)$$

With:

ρ = Density of the air (kg/m^3)
A = Cross-sectional area of the wind (m^2)
V = velocity of the wind (m/s)

Figure 12. ASC Power Consumption.

The figure above is the power consumption data taken directly by measurement at the port location where the ASC is located. This data shows that the average overall power consumption of the ASC is 230,109 Watts with an average power consumption per ASC unit per day is 7,670 Watts. This data is also supported by the calculation in equation (13) multiplied by the amount of efficiency from equation (12) which shows information that one wind turbine with an axial flux permanent magnet generator can produce 88,497 Watts per day. Furthermore, it can be said that one wind turbine can supply 12 ASC units at once.

4.5. Torque Output

Torque in a vertical axis wind turbine (VAWT) is generated through the interaction between the turbine blades and the wind flowing through them [42]. When the wind hits the turbine blades, it generates aerodynamic forces consisting of lift and drag. The lift generated by the blades moving along the wind flow tends to push the blades, creating a torsional moment on the turbine shaft. In addition, drag also contributes, although usually in the opposite direction to lift [43]. During rotation, the angle of attack of the blades against the wind is constantly changing, affecting the amount of lift and drag generated. The combination of these forces creates a torque that causes the turbine to rotate. This torque is then converted into mechanical power that can be converted into electrical power by a generator connected to the turbine.

$$RPM = 60 \times v \times \frac{TSR}{\pi \times D} \tag{14}$$

By entering the parameter values TSR = 5, π = 3.14, then the diameter of turbine D = 0.75 m, so that the torque obtained is 1,655 rpm for a wind speed of 13 m/s and 891 rpm for a wind speed of 7 m/s. For the maximum wind speed, the torque value obtained is greater than the assumed value used. This is certainly a good thing because the turbine can work more optimally with a maximum torque value.

4.6. Cost Efficiency Calculation

Based on PT Perusahaan Listrik Negara (PLN) policy, the electricity tariff class for medium government purposes (P-1/TR) with a power of 6,600 VA – 200 kVA is 1,699,53 rupiah per kWh according to Table 3.

Table 3. Electricity consumption price based on category and output power.

Category	Output Power	Price (Rp) /kWh
Small households (R1/TR)	900 VA	1,352,00
Small households (R1/TR)	1,300 VA	1,444,70
Small households (R1/TR)	2,200 VA	1,444,70
Medium households (R2/TR)	3,500VA– 5,500 VA	1,699,53
Large households (R3/TR)	≥ 6,600 VA	1,699,53
Medium business (B-2/TR)	6,600 VA – 200 kVA	1,444,70
Medium government (P-1/TR)	6,600 VA – 200 kVA	1,699,53
Public street lighting (P-3/TR)	> 200 kVA	1,699,53

Therefore, the power obtained from the calculation before is converted to 88.497 Watts hour. Then, to find out the benefits in terms of cost, this value needs to be converted into rupiah and multiplied by a certain time span. It was found that through the design of an axial flux permanent magnet generator, the cost incurred was Rp 4,510,692 per month and Rp 54,128,305 per year as shown in Table 4. This proves that there is a saving cost of 57.68% compared to the cost without an axial flux permanent magnet generator which costs Rp 7,819,111 per month and Rp 93,829,334 per year. This certainly is not a small number in a company's expenses. From that point, the application of axial flux permanent magnet generators in wind turbines to support ASC is absolutely needed.

$$kWh = \frac{P(w) \times T\ (hr)}{1000} \tag{15}$$

Table 4. Consumption cost.

Time	Cost
30 days	Rp 4,510,692
365 days	Rp 54,128,305
3650 days	Rp 541,283,050

5. CONCLUSIONS

Automatic Stacking Cranes (ASCs) are crucial in modern port operations, performing lifting, shifting, and stacking operations to ensure container movement. They are complemented by yard panels, which integrate with the port's Terminal Operating System (TOS) for efficient container handling. However, ASCs rely on electricity from the national grid, which can be unstable and cause disruptions to other critical port equipment. Wind turbines, which harness wind kinetic energy, can address these challenges by generating electricity that can meet the diverse power needs of ASCs. This study investigates the optimal structural analysis of Axial Flux Permanent Magnet Generators (AFPMGs) to ensure efficient operation and calculate energy losses to determine the feasibility of wind turbine systems in supporting ASCs' power requirements. This approach represents an environmentally friendly solution for power supply without disrupting other equipment's operation. The study has resulted innovative wind turbine systems that can adapt to fluctuating wind directions, unlocking the full potential of wind energy, particularly in coastal regions with abundant wind resources.

In this design, it is found that the axial flux permanent magnet generator can produce 88,497 Watts of power that can support 12 yards panels on the 12 Automatic Stacking Cranes. That is a very reasonable benefit, where only 2 wind turbines are needed to be able to supply the main power more efficiently for one port which generally has 20 ASCs. The AFPMG also can produce an average rotational speed of 1,655 rpm which is greater than the assumed average rotational speed of 1,500 rpm that makes the turbine can convert more kinetic energy from the wind into the mechanical energy needed to turn the turbine shaft and ultimately generate more electricity. This is reinforced by calculation data related to electricity cost savings that occur amounting to 39,701,029 rupiah per year or equivalent to 57.68%. So therefore, the port only needs to spend around 4,510,692 rupiah per month, 54,128,305 per year, and 541,283,050 rupiah per 10 years for Automatic Stacking Crane which is certainly very profitable for the company.

REFERENCES

[1] J. Zhu and F. Ma, "Scheduling of twin automatic stacking cranes and automated guided vehicle considering buffer mode on automated container terminal," *Comput. Ind. Eng.*, vol. 193, p. 110271, 2024, doi: 10.1016/J.CIE.2024.110271.

[2] B. Lu, M. Zhang, X. Xu, C. Liang, Y. Wang, and H. Liu, "Container Yard Layout Design Problem with an Underground Logistics System," *Journal of Marine Science and Engineering*, vol. 12, no. 7, pp. 1103–1103, Jun. 2024, doi: https://doi.org/10.3390/jmse12071103.

[3] Richard, Angelia, and C. Holyson, "Integration Process Between Terminal Operating System and Enterprise Resource Planning System in State-owned Port Business," in *2019 IEEE 9th International Conference on System Engineering and Technology (ICSET)*, 2019, pp. 385–390. doi: 10.1109/ICSEngT.2019.8906464.

[4] C. S. Lai, X. Li, G. Locatelli, and L. L. Lai, "Cost benefit analysis and data analytics for renewable energy and electrical energy storage," in *The 11th IET International Conference on Advances in Power System Control, Operation and Management (APSCOM 2018)*, 2018, pp. 1–3. doi: 10.1049/cp.2018.1737.

[5] M. R. Wahid, B. A. Budiman, E. Joelianto, and M. Aziz, "A review on drive train technologies for passenger electric vehicles," *Energies*, vol. 14, no. 20, pp. 1–24, 2021, doi: 10.3390/en14206742.

[6] M. M. Putri, A. Rusdiansyah, and S. Nurminarsih, "Model of Twin Automatic Stacking Crane Operation Strategy with Dynamic Handshake Area in an Automated Container Terminal," *J. Tek. Ind.*, vol. 25, no. 1, pp. 79–96, 2023, doi: 10.9744/jti.25.1.79-96.

[7] G. Cortina, M. Calaf, and R. B. Cal, "Distribution of mean kinetic energy around an isolated wind turbine and a characteristic wind turbine of a very large wind farm," *Phys. Rev. Fluids*, vol. 1, no. 7, 2016, doi: 10.1103/PhysRevFluids.1.074402.

[8] R. Zoro and A. Purwadi, "The use of wind turbine structure for lightning protection system," in *Proceedings of the 2011 International Conference on Electrical Engineering and Informatics*, 2011, pp. 1–6. doi: 10.1109/ICEEI.2011.6021800.

[9] R. D. Wooten, "Statistical analysis of the relationship between wind speed, pressure and temperature," *J. Appl. Sci.*, vol. 11, no. 15, pp. 2712–2722, 2011, doi: 10.3923/jas.2011.2712.2722.

[10] H. Lu and S. Wang, "A study on multi-ASC scheduling method of automated container terminals based on graph theory," *Comput. Ind. Eng.*, vol. 129, no. January, pp. 404–416, 2019, doi: 10.1016/j.cie.2019.01.050.

[11] C. Lu and Z. Wang, "A Knowledge Based Rapid Design System for Crane Gantry," in *2010 International Conference on System Science, Engineering Design and Manufacturing Informatization*, 2010, pp. 249–252. doi: 10.1109/ICSEM.2010.74.

[12] V. Yaramasu, B. Wu, P. C. Sen, S. Kouro, and M. Narimani, "High-power wind energy conversion systems: State-of-the-art and emerging technologies," *Proc. IEEE*, vol. 103, no. 5, pp. 740–788, 2015, doi: 10.1109/JPROC.2014.2378692.

[13] O. Beik and A. Al-Adsani, "Wind Turbine Productivity and Wind Energy Assessment: An Ontario Case Study," in *2020 IEEE Electric Power and Energy Conference (EPEC)*, 2020, pp. 1–5. doi: 10.1109/EPEC48502.2020.9320110.

[14] A. Alarabi and M. E. El-Hawary, "Rotor angle wind turbine energy capture control," in *2015 IEEE 28th Canadian Conference on Electrical and Computer Engineering (CCECE)*, 2015, pp. 444–451. doi: 10.1109/CCECE.2015.7129318.

[15] J. Y. Lee, J. H. Lee, and T. K. Nguyen, "Axial-flux permanent-magnet generator design for hybrid electric propulsion drone applications," *Energies*, vol. 14, no. 24, 2021, doi: 10.3390/en14248509.

[16] R. CHAVAN, G. RUPALI, and N. A.-E. R. and Technology, "Manufacturing Of Axial Flux Permanent Magnet Generator," *Neliti.Com*, vol. 6, no. 4, pp. 49–55, 2019, [Online]. Available: https://www.neliti.com/publications/428453/manufacturing-of-axial-flux-permanent-magnet-generator

[17] A. Parviainen, J. Pyrhönen, and P. Kontkanen, "Axial flux permanent magnet generator with concentrated winding for small wind power applications," *2005 IEEE Int. Conf. Electr. Mach. Drives*, no. May, pp. 1187–1191, 2005, doi: 10.1109/iemdc.2005.195871.

[18] D. H. Al-Janan and M. I. Saputra, "Optimasi Desain Sudu Turbin Dengan Paduan Savonius Dan Darrieus Untuk Meningkatkan Daya," *J. Rekayasa Mesin*, vol. 14, no. 2, pp. 677–687, 2023, doi: 10.21776/jrm.v14i2.1430.

[19] C. Zhao, J. Luo, S. Xie, and H. Li, "Experiment validation of vertical axis wind turbine control system based on wind energy utilization coefficient characteristics," in *2015 IEEE International Conference on Cyber Technology in Automation, Control, and Intelligent Systems (CYBER)*, 2015, pp. 1640–1644. doi: 10.1109/CYBER.2015.7288191.

[20] Evan Shahriar, Md. Mainuddin Sagar, Md. Rezwan Alam, and Kazi Afzalur Rahman, "Design and fabrication of a helical vertical axis wind turbine for electricity supply," *World J. Adv. Eng. Technol. Sci.*, vol. 12, no. 1, pp. 201–217, 2024, doi: 10.30574/wjaets.2024.12.1.0205.

[21] Ismail, E. Pane, and Triyanti, "Optimasi Perancangan Turbin Angin Vertikal Tipe Darrieus Untuk Penerangan Di Jalan Tol," *Semin. Nas. Sains dan Teknol.*, vol. 1, no. November, p. 12, 2017.

[22] L. Bisenieks, D. Vinnikov, and I. Galkin, "New converter for interfacing PMSG based small-scale wind turbine with residential power network," *2011 7th Int. Conf. Compat. Power Electron. CPE 2011 - Conf. Proc.*, no. July, pp. 354–359, 2011, doi: 10.1109/CPE.2011.5942260.

[23] A. Jamaldi, A. H. Purwono, D. Andriyansyah, and E. B. Raharjo, "Pengaruh Jumlah Sudu Terhadap Kinerja Turbin Savonius Tipe Drag Pada Aliran Air Dalam Pipa," *J. Rekayasa Mesin*, vol. 15, no. 1, pp. 73–82, 2024, doi: 10.21776/jrm.v15i1.1338.

[24] J. . Herbst and J. . Croat, "Neodymium-iron-boron permanent magnets J.F.," vol. 100, pp. 57–78, 1991.

[25] P. Irasari and N. Idayanti, "Aplikasi Magnet Permanen BaFe12 O19 dan NdFeB Pada Generator Magnet Permanen Kecepatan Rendah Skala Kecil," *Indones. J. Mater. Sci.*, vol. 11, no. 1, pp. 38–41, 2009.

[26] S. R. Trout and Y. Zhilichev, "Effective use of neodymium iron boron magnets, case studies," *Proc. - Electr. Insul. Conf. Electr. Manuf. Coil Wind. Conf. EEIC 1999*, no. February 1999, pp. 437–440, 1999, doi: 10.1109/EEIC.1999.826249.

[27] M. Qian, N. Chen, L. Zhao, D. Zhao, and L. Zhu, "A new pitch control strategy for variable-speed wind generator," in *IEEE PES Innovative Smart Grid Technologies*, 2012, pp. 1–7. doi: 10.1109/ISGT-Asia.2012.6303274.

[28] M. R. Wahid, E. Joelianto, and N. A. Azis, "System Identification of Switched Reluctance Motor (SRM) Using Black Box Method for Electric Vehicle Speed Control System," in *2019 6th International Conference on Electric Vehicular Technology (ICEVT)*, 2019, pp. 208–212. doi: 10.1109/ICEVT48285.2019.8994020.

[29] A. Fajar, "Rancang Bangun Generator Sinkron Axial Flux Permanent Magnet

1500 Watt," *J. Tek. Energi*, vol. 5, no. 33, pp. 18–36, 2017.

[30] T. Gundogdu, Z. Q. Zhu, and J. C. Mipo, "Influence of stator slot and pole number combination on rotor bar current waveform and performance of induction machines," in *2017 20th International Conference on Electrical Machines and Systems (ICEMS)*, 2017, pp. 1–6. doi: 10.1109/ICEMS.2017.8055937.

[31] J. F. Gieras, R. J. Wang, and M. J. Kamper, *Axial Flux Permanent Magnet Brushless Machines*.

[32] Y. Guan *et al.*, "Influence of Pole Number and Stator Outer Diameter on Volume, Weight, and Cost of Superconducting Generators With Iron-Cored Rotor Topology for Wind Turbines," *IEEE Trans. Appl. Supercond.*, vol. 27, no. 6, pp. 1–9, 2017, doi: 10.1109/TASC.2017.2716818.

[33] S. Khan, S. Amin, and S. S. Hussain Bukhari, "Design and Comparative Performance Analysis of Inner Rotor and Inner Stator Axial Flux Permanent Magnet Synchronous Generator for Wind turbine Applications," in *2019 2nd International Conference on Computing, Mathematics and Engineering Technologies (iCoMET)*, 2019, pp. 1–7. doi: 10.1109/ICOMET.2019.8673537.

[34] F. Danang Wijaya, N. A. Rahadyan, and H. R. Ali, "Magnetic flux distribution due to the effect of stator-rotor configuration in the axial machine," in *2014 6th International Conference on Information Technology and Electrical Engineering (ICITEE)*, 2014, pp. 1–6. doi: 10.1109/ICITEED.2014.7007941.

[35] M. Muteba, "Influence of Mixed Stator Winding Configurations and Number of Rotor Flux-Barriers on Torque and Torque Ripple of Five-Phase Synchronous Reluctance Motors," in *2019 IEEE Transportation Electrification Conference and Expo (ITEC)*, 2019, pp. 1–6. doi: 10.1109/ITEC.2019.8790614.

[36] Z. Wen, L. Ruan, and G. Gu, "Optimum Design of Hollow Conductor in Stator Winding for Large Evaporative Hydro-generator," in *2006 CES/IEEE 5th International Power Electronics and Motion Control Conference*, 2006, pp. 1–4. doi: 10.1109/IPEMC.2006.4777971.

[37] F. Meguellati and F. Ferroudji, "Aerodynamic Analysis of an H-Type VAWT Rotor for Different Symmetrical NACA 00xx Airfoils," in *2023 Second International Conference on Energy Transition and Security (ICETS)*, 2023, pp. 1–3. doi: 10.1109/ICETS60996.2023.10410699.

[38] A. Kuthi, J. M. Sanders, and M. A. Gundersen, "Core and copper loss effects on the stepped impedance transmission line pulse generator," in *2016 IEEE International Power Modulator and High Voltage Conference (IPMHVC)*, 2016, pp. 22–25. doi: 10.1109/IPMHVC.2016.8012919.

[39] L. Mihet-Popa and V. Groza, "Annual wind and energy loss distribution for two variable speed wind turbine concepts of 3 MW," in *2011 IEEE International Instrumentation and Measurement Technology Conference*, 2011, pp. 1–5. doi: 10.1109/IMTC.2011.5944340.

[40] W. Liu, J. Chen, C. Zhang, Z. Cui, and X. Wang, "Ventilation system design and rotor air friction loss of high-speed permanent magnet machines," in *2017 IEEE International Conference on Cybernetics and Intelligent Systems (CIS) and IEEE Conference on Robotics, Automation and Mechatronics (RAM)*, 2017, pp. 310–315. doi: 10.1109/ICCIS.2017.8274793.

[41] I. O. Bucur, I. Mălăel, and M. Predescu, "Predesign and Aerodynamic Efficiency Evaluation of a VAWT adapted to Romania Wind Conditions," in *2019 International Conference on ENERGY and ENVIRONMENT (CIEM)*, 2019, pp. 29–33. doi: 10.1109/CIEM46456.2019.8937644.

[42] L. Gumilar, M. A. Habibi, D. Prihanto, H. Wicaksono, J. R. Larasati, and A. Gunawan, "Analysis curve of maximum power and torque turbine generated by vertical axis wind turbine based on number of blades," *AIP Conf. Proc.*, vol. 2217, no. April, 2020, doi: 10.1063/5.0000709.

[43] K. S. Park, T. Asim, and R. Mishra, "Numerical investigations on the effect of blade angles of a vertical axis wind turbine on its performance output," *Int. J. COMADEM*, vol. 18, no. 3, pp. 3–10, 2015.